Behavior of Reinforced Concrete Continuous Deep Beams in Shear

Fouad B.A. Beshara, Ibrahim G. Shaaban, and Tarek S. Mustafa
Civil Engineering Department
Banha University, Faculty of Engineering at Shobra
Cairo – Egypt

ABSTRACT

Test results of nine reinforced concrete continuous deep beams are presented and analyzed. The main variables studied were shear span-to- depth ratio (a/d), vertical web reinforcement ratio (ρ_v), horizontal web reinforcement ratio (ρ_h), and concrete compressive strength (f_{cu}). The results of this study show that the stiffness reduction was prominent in case of lower concrete strength and higher shear span-to depth ratio and that the variation of strains along the main longitudinal top and bottom bars was found to be dependent on the shear span-to depth ratio. For beams having small (a/d) ratio, horizontal shear reinforcement was always more effective than vertical shear reinforcement. Finally, the obtained test results are compared to the predictions of finite element analysis using the ANSYS 10 program and a well agreement between the experimental and analytical results was found.

Keywords: continuous beams; deep beams; deflection; reinforced concrete; shear strength; web reinforcement.

1- INTRODUCTION

Reinforced concrete (RC) continuous deep beams are fairly commonly used as load distribution elements such as transfer girders, pile caps, tanks, folded plates, and foundation walls, often receiving many small loads and transferring them to a small number of reaction points. There have been extensive experimental investigations of simply supported RC deep beams [1-11], but very few tests to our knowledge, are performed on continuous RC deep beams. [12-16]. Continuous deep beams differ from either simply supported deep beams or continuous shallow beams. In continuous deep beams, the regions of high shear and high moment coincide and failure usually occurs in these regions. In simple RC deep beams, the region of high shear coincides with the region of low moment. Failure mechanisms for continuous RC deep beams are therefore significantly different from failure mechanisms in simply supported RC beams. Deep

beams develop a truss or tied arch action more marked than in shallow beams where shear is transferred through a fairly uniform diagonal compression field.

The present paper reports test results of nine two-span RC deep beams [17]. The tested variables were shear span-to-depth ratio, vertical web reinforcement ratio, horizontal web reinforcement ratio, and concrete compressive strength. The specimens were tested in a compression machine where increasing monotonic static loads were at each mid-span. All tested beams were loaded until failure. The failure planes evolved along the diagonal crack formed at the concrete strut along the edges of the load and intermediate support plates. The test results were measured at different loading levels for the mid-span deflection, mid-span bottom steel strain, middle-support top steel strain, middle-support stirrups strain, and end-support stirrups strain. Also, the cracking patterns were identified. The effects of testing variables on the first diagonal crack load, ultimate shear load, deflection, stiffness, and failure mechanisms were studied. Finally, the obtained test results are compared to the predictions of finite element analysis for continuous deep RC beams.

2- EXPERIMENTAL PROGRAM

2-1 Test Specimens and Materials

Nine two-span RC deep beams were tested. The overall dimensions of each series are shown in Fig. 1. All tested beams had the same span length and width. The overall length L was 2000 mm divided by two spans of 1000 mm for each and the width b was 150 mm. The locations of center lines of loads and supports were the same for all tested beams. According to the beam height (h) and shear span-to-depth (a/d) ratios, the beams were divided into three groups. For tested beams (BS1, BS2, BS3, BS6, and BS9), the height was 500 mm and (a/d) ratio was one. For tested beams (BS4, BS5, and BS7) the height was 650 mm and (a/d) ratio was 0.77. The height of last beam (BS8) was 400 mm to give (a/d) ratio as 1.25. The details of reinforcement and height for each beam are shown in Fig. 2 and Table (1), respectively. The main longitudinal top and bottom reinforcement was sufficient and kept constant for all tested beams in order to prevent premature flexural failure. All longitudinal bottom steel reinforcement extended the full length of the beams and through the depth to provide sufficient anchorage lengths. The vertical web reinforcement was closed stirrups and the horizontal web reinforcement as longitudinal bars in both sides of the beam. All longitudinal top and bottom reinforcement was 16-mm diameter high-strength steel bars with yield stress of 400 MPa. The web reinforcement was normal mild steel of 8-mm diameter with yield stress of 280 MPa. The amount of vertical and horizontal web reinforcement included three levels. Several trial mixes have been tested to achieve the target compressive concrete strengths of 25 MPa and 35 MPa at 28 days with water/cement ratio (w/c) of 0.6 and 0.475, respectively.

2-2 Testing Procedure and Instrumentation

Figure 3 shows the test setup. Special arrangements had been taken to obtain two point loads and three support reactions. A top steel spreader beam was used to divide the total applied load from the machine head into two equal point loads, one in each span.

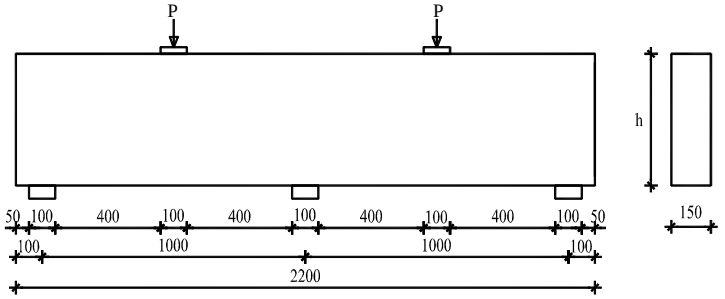

Fig. 1. Geometrical Dimensions of the Tested RC Deep Beams (mm)

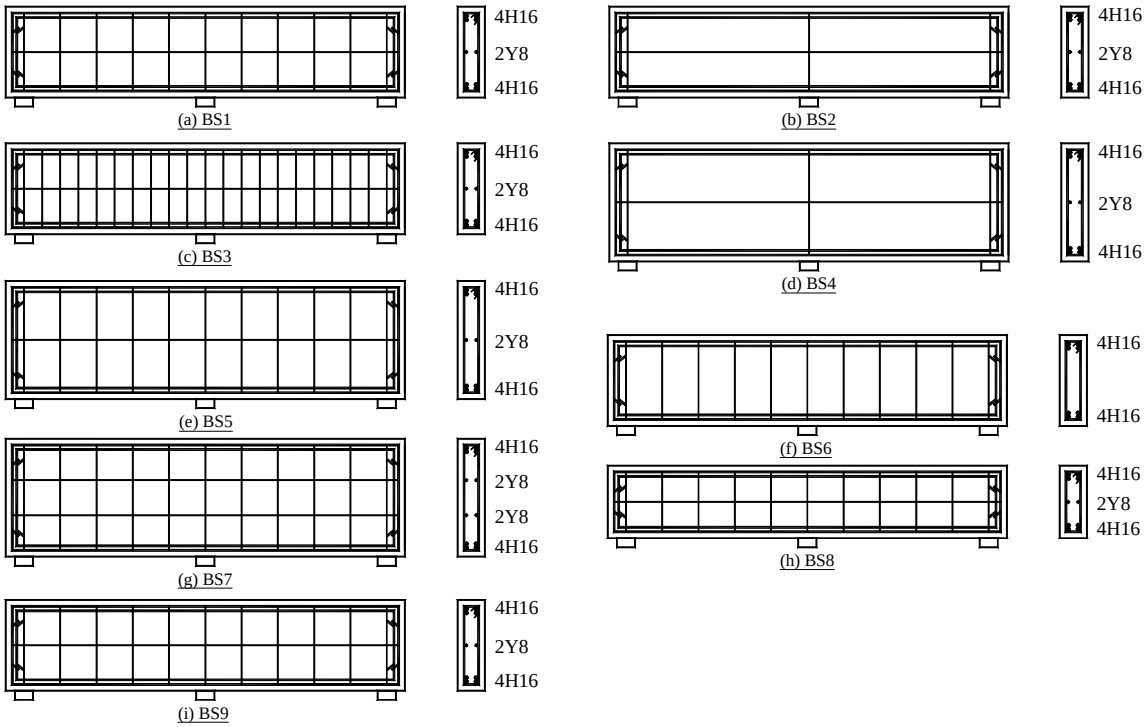

Fig. 2. Details of Tested RC Deep Beams

Table (1) Details of Reinforcement for the Tested Beams

BEAM	h (mm)	(a/d)	VL RFT	ρ_v (%)	HL RFT	ρ_h (%)	f_{cu}(MPa)
BS1	500	1	Y8@200	0.33	2Y8	0.33	25
BS2	500	1	0	0.0	2Y8	0.33	25
BS3	500	1	Y8@100	0.66	2Y8	0.33	25
BS4	650	0.77	0	0.0	2Y8	0.24	25
BS5	650	0.77	Y8@200	0.33	2Y8	0.24	25
BS6	500	1	Y8@200	0.33	0	0.0	25
BS7	650	0.77	Y8@200	0.33	4Y8	0.48	25
BS8	400	1.25	Y8@200	0.33	2Y8	0.44	25
BS9	500	1	Y8@200	0.33	2Y8	0.33	35

Another stiffer steel beam was placed underneath the tested beams to collect the three support reactions to the other head of the machine. Each beam was tested as a continuous beam under two vertical concentrated loads using a vertical hydraulic jack. The three supports rested on flat plates to combat instability out of the beam plane as shown in Fig. 3. All tested beams were painted by a thin white coat to facilitate the observation and determination of cracks at different stages of loading. With regard to the two vertical loads, they were similar in their acting position, value and were separated by a distance equal 1000 mm. During testing, the vertical loads were applied in increments equal to about 5% of the expected ultimate load and up to failure. After each load increment, marking of cracks was made and the results were recorded automatically using the data logger.

The loads and reactions have been measured using a load cell of capacity 2000 kN and 0.1 kN accuracy. The load cell readings were recorded automatically using the data logger. The corresponding vertical deflections of test beams at the locations of the mid-span point were measured using LVDT's of 100 mm capacity and 0.01 mm accuracy. Electrical strain gauges of length 10 mm, with resistance 120.4 ± 0.4 ohm, and a gauge factor of 2.11 were used to measure the strains in the main longitudinal top and bottom flexural steel, vertical stirrups, and horizontal shear reinforcement. The gauges were fixed on the steel bars before casting. The surface of the steel was cleaned and smoothed, and the gauges were installed on the steel bars using adhesive material and then they were covered with a water proofing material for protection. For all beams, two gauges were fixed on the top bar at the interior support and on the bottom bar at the mid span. In addition, four gauges were fixed on two vertical stirrups and horizontal shear reinforcement at intersection points of these stirrups and horizontal reinforcement with the strut lines joining the point load with the internal and external supports. The load, deflections, and steel strains were measured and recorded automatically by connecting the load cell, LVDT's, and the electrical strain gauges to data acquisition system.

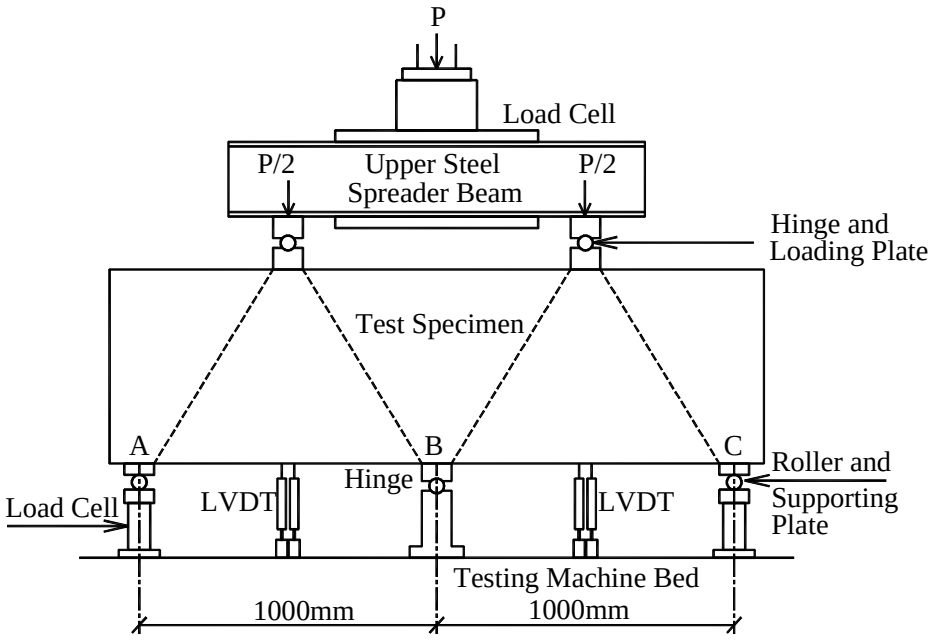

Fig. 3. Typical Test Setup and Instrumentation for all Tested Beams

3- EXPERIMENTAL RESULTS

3-1 Specimen Behavior

Figure 4 shows the cracking patterns at failure for the tested beams (BS1, BS4, and BS8) with (a/d) of 1.0, 0.77, and 1.25 respectively. In the figure, each crack is marked by a line representing the direction of cracking. The crack propagation was significantly influenced by the (a/d) ratio as shown in Fig. 4. Specimens with larger (a/d) showed earlier development of flexural cracks, and a less well defined shear cracks. Generally, the first crack suddenly developed in the flexural sagging region at approximately 25% of the ultimate strength, and then a crack in the diagonal direction at approximately 30% of the ultimate strength at the mid-depth of the concrete strut within the interior shear span immediately followed. The first flexural crack over the intermediate support generally occurred at approximately 80% of the ultimate strength. As the load increased, more flexural and diagonal cracks were formed and a major diagonal crack extended to join the edges of the load and intermediate support plates. A diagonal crack within the exterior shear span occurred suddenly near the failure load. Just before failure, the two spans showed nearly the same crack patterns. All tested beams developed the same mode of failure as observed in [13]. The failure planes were traced along the diagonal crack formed at the concrete strut along the edges of the load and intermediate support plates. Two rigid blocks separated from original beams at failure due to the significant diagonal cracking. The influence of shear reinforcement on the tested beams behavior was not significant as mentioned before in [13,14]. In beam without stirrups (BS2), the failure was sudden and was due to crushing of the concrete compression struts. When sufficient stirrups are present, crack fans develop under the loads, and over the interior support; these cracks diminish the effective width of any direct compression strut which might develop.

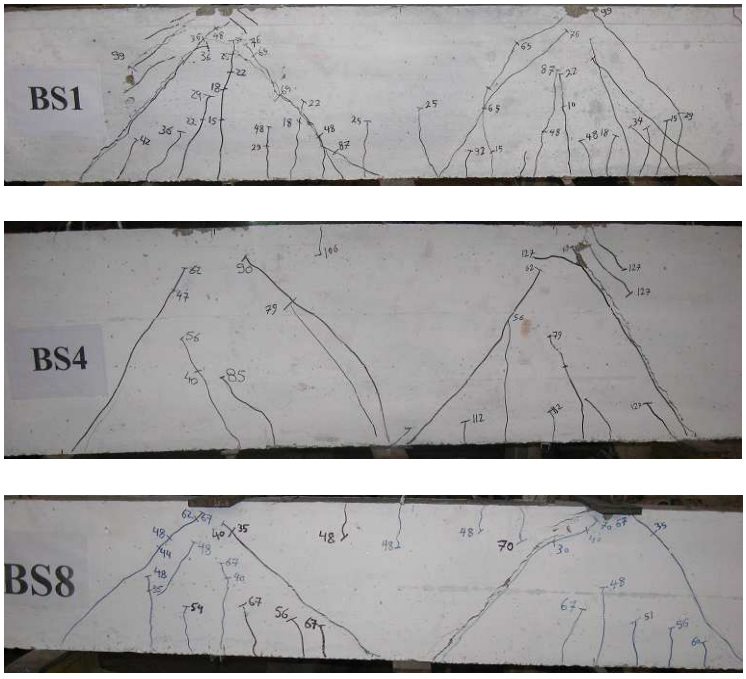

Fig. 4. Crack Patterns and Failure Zones of Tested Beams BS1, BS4, and BS8

3-2 Mid-Span Deflections

The measured load-deflection curves for all tested beams are shown in Fig. 5. Also, the measured first flexural cracking load at mid-span (P_{crfm}), the first flexural cracking load at internal support (P_{crfs}), the first diagonal cracking load (P_{crs}), and the ultimate total load (P_u) are given in Table (2).

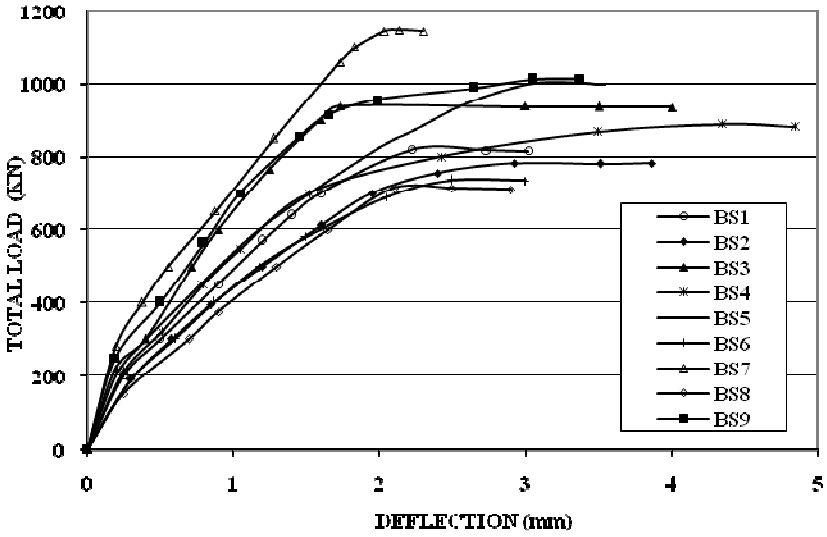

Fig. 5. Total Applied Load and Mid-Span Deflection Relationship of the Tested Beams

Table (2) Experimental Results of the Tested Beams

BEAM	BS1	BS2	BS3	BS4	BS5	BS6	BS7	BS8	BS9
P_{crfm}(kN)	200	200	250	300	320	200	370	150	250
P_{crfs} (kN)	600	585	660	680	740	550	860	540	750
P_{crs} (kN)	250	240	280	290	340	240	390	220	300
P_u (kN)	819	782	939	889	1001	735	1145	715	1015
R_{outer} (kN)	148	141	169	161	181	133	206	129	183
R_{inner} (kN)	523	500	601	567	639	469	733	457	649
Q_{uinner} (kN)	262	250	301	284	320	235	367	229	325
Q_{uACI} (kN)	215	201	255	267	280	175	350	174	245
Q_{uECP} (kN)	204	191	218	262	277	173	330	169	238

It can be seen from Fig. 5 and Table (2) that the decrease of (a/d) leads to an increase in the load carrying capacity and stiffness of tested beams at different levels. The measured deflections indicate that beams with smaller (a/d) ratio exhibit less deformation and ductility than that of higher (a/d) ratio, and as (a/d) ratio decreased; the deflection at the same load level is reduced. Increasing (a/d) ratio from 1.0 for beam

BS1 to 1.25 for beam BS8 resulted in a decrease in P_{crfm}, P_{crs} and P_u by about 25.0%, 12.0%, and 13.0%, respectively. Furthermore, the enhancement in P_{crfm}, P_{crs} and P_u is respectively 60.0%, 36.0%, and 22.0% due to decreasing (a/d) ratio from 1.0 for beam BS1 to 0.77 for beam BS3. It can be seen that increasing the concrete compressive strength has a significant improvement effect on the load-deflection response. Increasing the concrete compressive strength led to a more brittle behavior with increased load carrying capacities and stiffness at different load levels. The P_{crfm}, P_{crs} and P_u were increased respectively by 25.0%, 20.0%, and 24.0% for beam BS9 with (f_{cu}) of 35.0 MPa when compared to beam BS1 with (f_{cu}) of 25.0 MPa.

The examination of measured results in Fig. 5 and in Table (2) showed that the load carrying capacities at different levels increase with an increase in the ratio of vertical shear reinforcement (ρ_v). The tested beam BS2 without stirrups showed a minor reduction in P_{crs} and P_u by 4.0% and 5.0% when compared to beam BS1(ρ_v= 0.0033), while the first flexural cracking load was kept the same. On the other hand, the increase in P_{crfm}, P_{crs} and P_u was found 25%, 12.0%, and 15.0% respectively for beam BS3 having (ρ_v) as 0.0066 when compared to beam BS1with ρ_v= 0.0033. Figure 5 also indicates that beam without vertical stirrups had very little ductility, but tested continuous deep beams with heavy stirrups were ductile while those with light stirrups were fairly brittle.

The horizontal shear reinforcement has generally a moderate effect on the improvement of the measured load-deflection response of tested deep beams. From comparison of results in Fig. 5 and Table (2), it was found that there is a reduction in P_{crs} and P_u by 4% and 10% respectively for tested beam BS6 with (ρ_h) of 0.00 when compared to beam BS1 with (ρ_h) of 0.0033 with the same (a/d) while the first flexural cracking load was found the same for both beams. In other comparison, beam BS7 with (ρ_h) of 0.0048 showed an increase in P_{crfm}, P_{crs} and P_u by 16.0%, 15.0%, and 14.5% respectively when compared to beam BS5 with (ρ_h) of 0.0024 while the other parameters were kept constant.

3-3 Steel Strains

Figures 6 and 7 show the load-steel strain curves for bottom and top longitudinal flexural reinforcement of the tested beams. These figures also indicate that tested beams with the same (a/d) ratio shows almost the same total applied load-strain gradient with major strains redistribution in the bottom steel after the first diagonal cracking. The total applied load-strain gradient shows minor strains redistribution in the top steel after the first diagonal cracking and shows also the same similarity for the beams with the same (a/d) ratio. The bottom longitudinal reinforcement was in tension throughout the length of the beam, and the top reinforcement was also in tension throughout the length of the interior shear span. Neither bottom nor top longitudinal flexural reinforcement was yielded up to failure load for the tested beams due to the over reinforced design of flexural reinforcement. Strains in bottom reinforcement were higher than in top steel due to stress redistribution which increases the field moment and decreases the moment at the middle support. In beam without stirrup (BS2), the flexural reinforcement strains are constant along the bars between point loads and supports and a compression struts develop in the concrete which carry the loads directly to the supports.

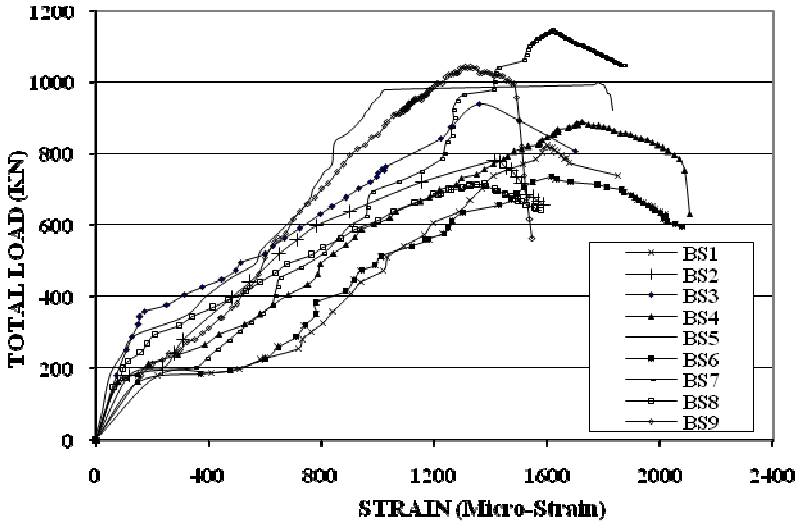

Fig. 6. Total Applied Load and Bottom Steel Strain Relationship for the Tested Beams

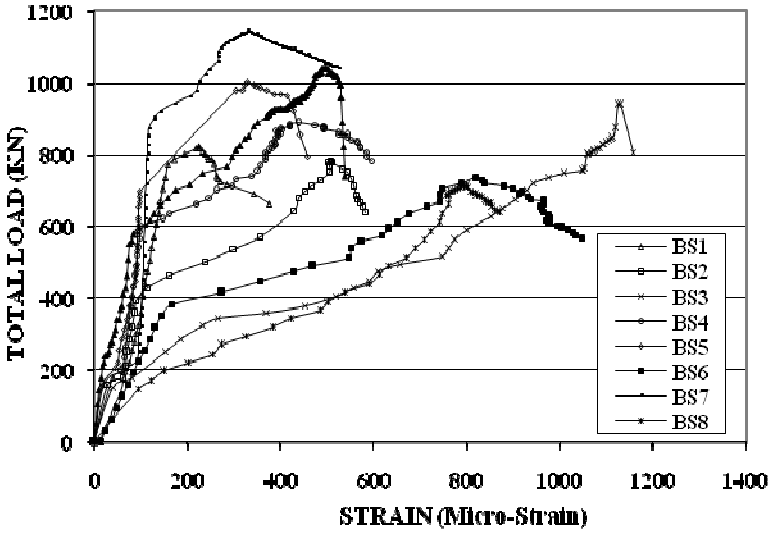

Fig. 7. Total Applied Load and Top Steel Strain Relationship for the Tested Beams

The total load-steel strain curves for vertical and horizontal shear reinforcement at the interior shear span for the tested beams are shown in Figures 8 and 9, respectively. A minor redistribution of strains occurred at the vertical steel after the occurrence of the first diagonal crack for the beams BS5 and BS1 having the lower values of (a/d) ratio as 0.77 and 1.0 respectively and did not yield. A major strain redistribution occurred for beam BS8 having (a/d) ratio of 1.25 and reached yield at failure. For the horizontal steel, a redistribution of strains occurred after first diagonal cracking for these three beams but this redistribution was higher for beam BS5 having the lowest (a/d) ratio of 0.77. None of the horizontal reinforcement for the three test beams reached yield up to failure. Comparison of test results indicate that the influence of web steel on the ultimate shear strength is influenced by the (a/d) ratio, the lower the (a/d) ratio; the more effective the horizontal steel and the less effective the vertical steel. Only the vertical steel of beam BS3 having a heavy vertical steel ratio reached yield.

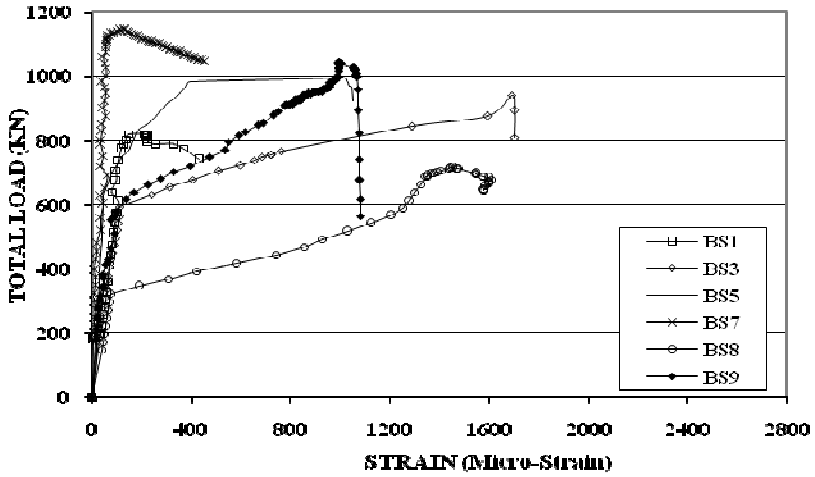

Fig. 8. Total Applied Load and Vertical Shear Reinforcement Strain Relationship

It was also concluded that tested beam BS6 without horizontal reinforcement showed a higher values of strains in the vertical reinforcement than beam BS1 with (ρ_h) of 0.0033 at the same load level. A major redistribution of strains occurred for the vertical steel at about 70.0% of the ultimate load for beam BS9 but did not yield as the vertical reinforcement for beam BS1.

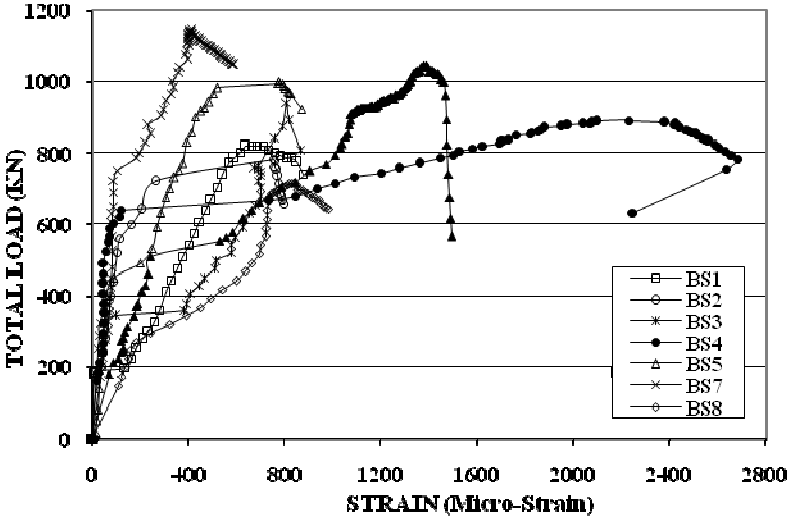

Fig. 9. Total Applied Load and Horizontal Shear Reinforcement Strain Relationship

For the horizontal reinforcement, while major strain redistribution was occur for beam BS1 at the first diagonal cracking, similar strain redistribution have been occurred in beam BS9 with higher value of (f_{cu}) but at about 50.0% of the ultimate load and this is due to the expected higher value of concrete shear contribution. Horizontal steel for beam BS9 almost reached yield point while beam BS1 did not reach that point.

3-4 Reaction of Supports

The measured amount of load transferred to the end support is listed in Table (2) for all tested beams. From external equilibrium of forces and symmetry, the measured reaction at intermediate support is evaluated in the table. Linear elastic analysis was performed

using "SAP" program for beams in order to assess the reactions of supports. From elastic analysis, the reactions of the exterior and intermediate supports due to the total applied load (P) are 0.175P and 0.65P respectively. It was stated before [12-15] that the differential settlement had no significant effect on the elastic behavior of continuous deep beams, and would have less significance at higher loads in any case. Figure 10 shows the measured amount of the load transferred to the end and intermediate supports against the total applied load for beams having constant (a/d) value of 1.0 and different web reinforcement ratios. On the same figure, the reactions at support are obtained from elastic analysis are also presented. Although the amount of web steel influences the maximum reaction at support, it has no effect on the total load-support reaction gradient. Before the first diagonal crack, the relationship of the end and intermediate support reactions against the total applied load in all tested beams shows good agreement with elastic prediction. The amount of loads transferred to the end support, however, was slightly higher than that predicted by the elastic analysis after the occurrence of the first diagonal crack within the interior shear span. At failure, the difference between the measured end support reaction and prediction of the elastic analysis was in order of 8%, 10%, and 14%, for beams with (a/d) of 0.77, 1.0, and 1.25, respectively. Therefore, the internal redistribution of forces is limited. Also, the distribution of applied load to supports is independent of the amount and configuration of shear reinforcement. This means that the occurrence of diagonal cracks reduces the beam stiffness and the hogging moment over the central support, and increases the sagging bending moment within the span.

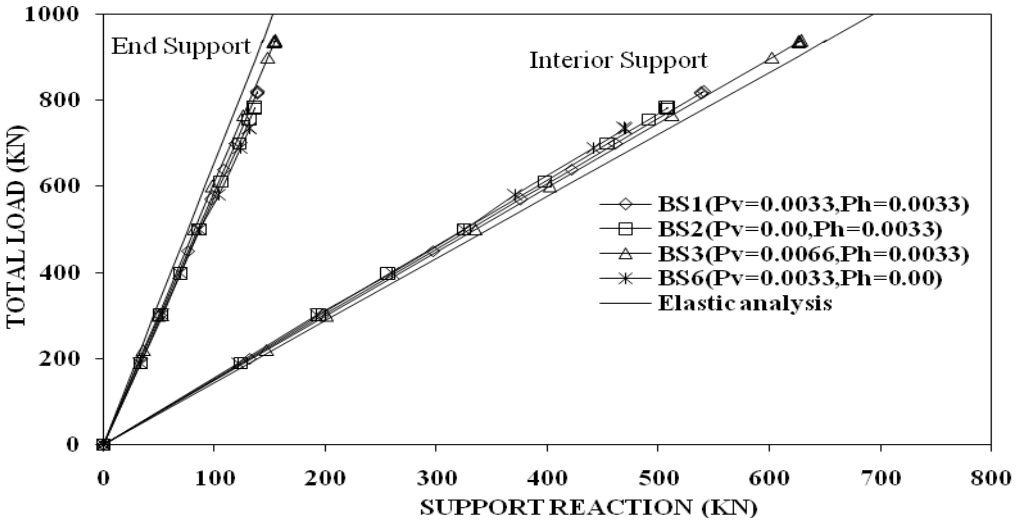

Fig. 10. Total Applied Load Versus Support Reactions for Beams having (a/d=1.0)

3-5 Experimental Shear Force Capacities and Comparison with Current Codes

The most critical shearing force in continuous deep beams occurs at the interior support. The shear forces at inner supports of tested deep beams (Q_{uinner}) are calculated as half the vertical support reactions, and are listed in Table (2). It can be seen that the ultimate shear strength of beams with constant shear reinforcement and concrete strength increase significantly with the decrease of (a/d) ratio. The decrease of (a/d) ratio from 1.25 (beam BS8) to 1.0 (beam BS1) increases the shear capacity by 14.4%. For beams

with vertical shear steel, the drop of (a/d) ratio from 1.0 (beam BS1) to 0.77 (beam BS5) enhances the shear capacity by 22.1%. For tested deep beams without vertical shear reinforcement, the drop of (a/d) ratio from 1.0 (beam BS2) to 0.77 (beam BS4) enhances the shear capacity by 13.6%. Table (2) indicates that the shear strength for beams with constant a/d ratio and shear reinforcement increases remarkably with the increase of concrete compressive strength. The shear capacity of beam BS9 with f_{cu}= 35 MPa is higher than that of beam BS1 with f_{cu}= 25 MPa by 24%. The analysis of experimental results indicates that the ultimate shear strength increases with the increase of amount of vertical or horizontal shear reinforcement for different (a/d) ratios. For tested beams with (a/d) ratio of 1.0, the increase of ρ_v from zero (beam BS2) to 0.0033 (beam BS1) and to 0.0066 (beam BS3) enhances the shear capacity by 5% and 20.4%, respectively. For tested beams (BS4 & BS5) with a/d= 0.77, the increase in ρ_v by 0.0033 increases the shear capacity by 12.7%. Previous test results of simple deep beams [7] have suggested that horizontal shear reinforcement has little effect on the shear strength improvement. In current test results, horizontal shear steel has a moderate effect on shear carrying capacity, especially for beams with a/d < 1. For beams (BS5 & BS7) with a/d= 0.77, the shear strength improvement was 14.7% due to 0.0024 increase in ρ_h ratio. For tested beams (BS1 & BS6) with a/d= 1, the same increase in ρh ratio improves the shear capacity by 12.7%.

The prediction of shear capacity of tested beams were shown in Table (2) using two design codes; namely ACI 318-08 [18] and the Egyptian concrete code of practice ECP-203-2007 [19]. The shear contributions from concrete, horizontal, and vertical shear reinforcement were evaluated with all safety factors removed. Both design methods show that the amount of shear resisted by horizontal steel is higher than that resisted by vertical steel (contrary to testing results). Figure 11 compares the obtained experimental results (Q_{uinner}), ACI predictions (Q_{uACI}), and ECP predictions (Q_{uECP}). The figure indicates that ACI as well as ECP underestimate the shear capacity for continuous deep beams. The average ratios of (Q_{uinner} / Q_{uACI}) and (Q_{uinner} / Q_{uECP}) are 1.21 and 1.27 with standard deviations of values 0.11 and 0.12, respectively. The discrepancy in codes predictions may be attributed to the fact that the shear strength equations in both design methods for continuous deep beams are derived from simple deep beam tests.

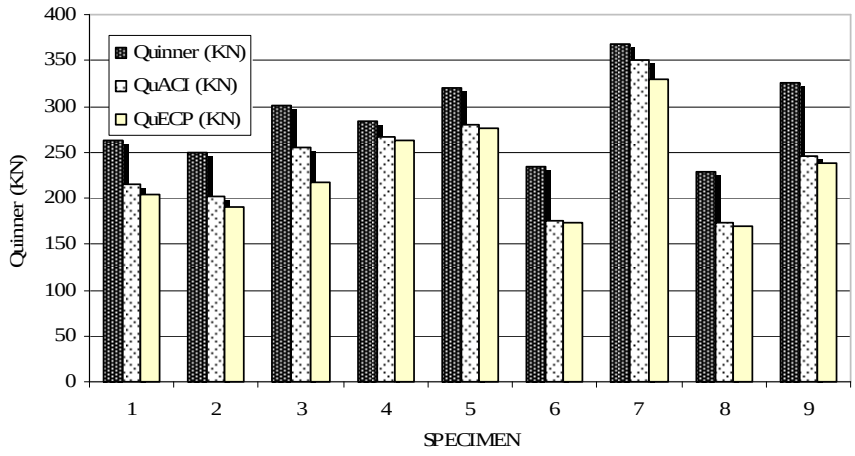

Fig. 11. Comparison between Experimental Ultimate Shear Capacity at Interior Support (Q_{uinner}) with ACI (Q_{uACI}) and ECP (Q_{uECP}) Design Equations

4- FINITE ELEMENT PREDECTIONS

The nonlinear finite element program; ANSYS 10 was used to predict the behavior of tested deep beams. A correlative study based on the load- deflection response as well as the cracking patterns was conducted to verify the analytical model with the obtained experimental results. In the finite element discretization of the tested beams, a 50x50 mm mesh of eight-node brick elements (Element 65) was used for concrete. The top & bottom flexural steel bars and the horizontal & vertical web reinforcement were represented by bar elements. The area and spacing of such bar elements were similar to the experimental specimens. The concentrated loads were also applied to the top surface at mid-span of the tested beams. The supports were represented by restrained nodes at the corresponding locations. To model concrete behavior, nonlinear stress-strain curves were used in compression and tension. Such models account for compression & tension softening, tension stiffening and shear transfer mechanisms in cracked concrete. An elasto-plastic model was used for steel in compression and tension. The initial Young's modulus in concrete was taken as 22 GPa; and the steel modulus was 200 GPa. An incremental-iterative technique was employed to solve the nonlinear equilibrium equations. The load increment was set at 5% of the experimental ultimate load. The load increment was subject to adjustment to obtain results at certain specific load levels. The maximum number of iterations was set to 20 in each load step and the equilibrium tolerance of 0.5% was chosen.

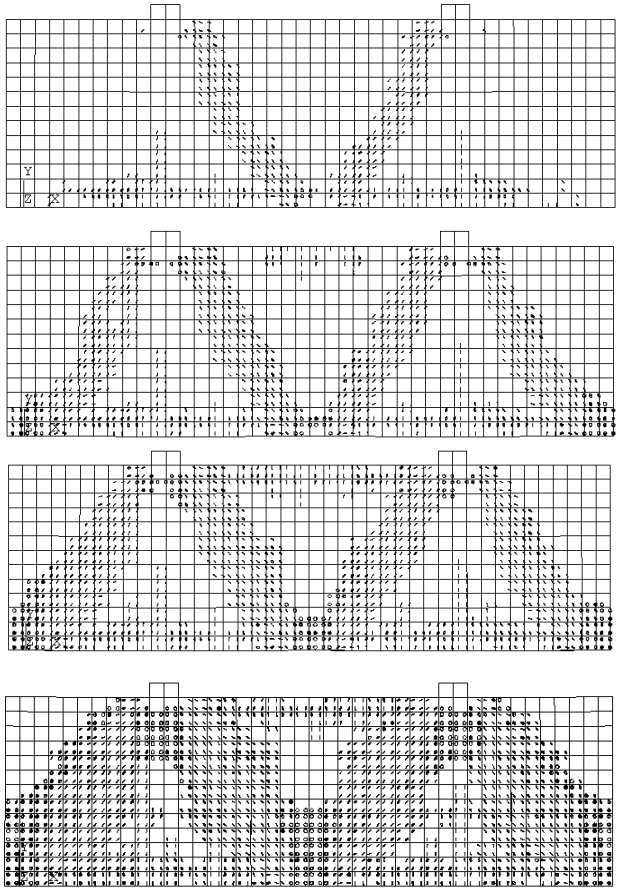

Fig. 12. Simulated Crack Propagation for Tested Beam BS5

The computed cracking patterns at different loading levels are presented for tested beams BS5 and BS8, respectively. Both specimens had the minimum amount of stirrups with (a/d) ratio as 0.77 and 1.25, respectively. Figure 12 shows the development of the crack pattern in tested beam BS5. First flexural cracking at mid-span (load level 250 kN) was predicted first by the simulation. Beyond this flexural crack, a shear crack band developed (load level 290 kN). After the formation of the crack band, a rather stable crack pattern is formed. The width of shear crack band increased with an increase of the load (load levels: 400-800 kN) in a stable manner. Later, flexural cracking takes place over the middle support. At ultimate stage, failure is initiated by crushing of the concrete in the region adjacent to the middle support (load level 910 kN). There is a good agreement between the simulated crack patterns and the obtained experimental ones. The simulation also successfully predicted the sequence in the crack patterns development and the failure mechanism.

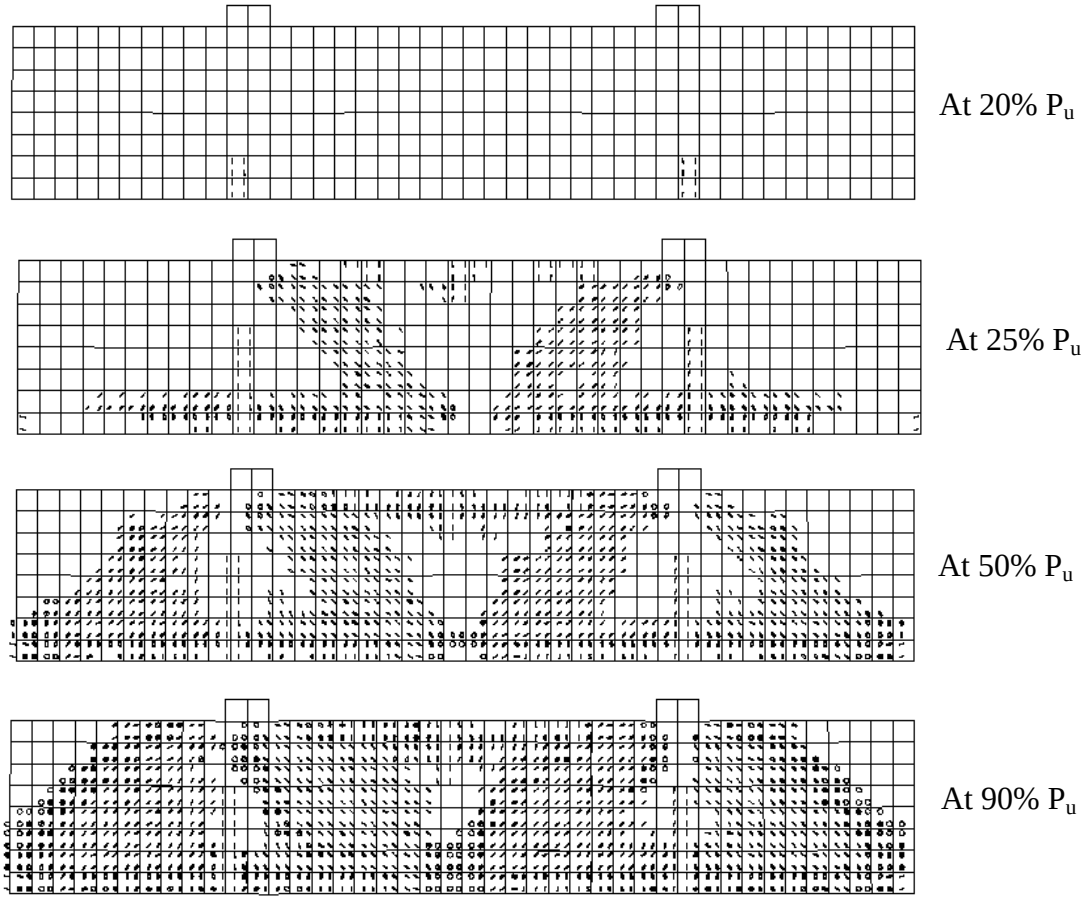

Fig. 13. Simulated Crack Propagation for Beam BS8

As shown in Fig. 13, the development of the crack pattern for tested beam BS8 with (a/d) ratio of 1.25 is nearly the same as that for tested beam BS5 with (a/d) ratio of 0.77. Compared to BS5, the load levels at which cracks takes place are lower due to increasing (a/d) ratio. First flexural cracking was firstly developed at the mid-span (load level 130 kN) and later over the middle support. At a load level of 170 kN, inclined flexural cracks develop. Afterwards, shear cracking takes place. With further load

increase, some secondary flexural cracks are detected. At ultimate stage, the deep beams failed by crushing of the concrete in the regions adjacent to the middle support and the loading point. The simulated and the experimental crack patterns are compared at ultimate load level and it is clear that the finite element analysis simulates the experiment results very well. This can be seen in the internal shear span; going from the middle support to the loading point, the crack direction changes from vertical to inclined, stays constant, and changes back to vertical again.

In Fig. 14, test results of total load- deflection curves are compared to the predictions of finite element analysis for tested beams BS1, BS2 and BS8. A good agreement between the experimental and analytical results was obtained at different levels. In simulated curves, there is a sudden increase in the deflection and this is back to formation of the first flexural crack. Also, formation of the first diagonal crack significantly reduced the beam stiffness. Similar to experimental results, simulated curves are significantly affected by the shear span-to-depth ratio. It can be seen from Fig. 14 that the decrease of (a/d) leads to an increase in the load carrying capacity at different levels.

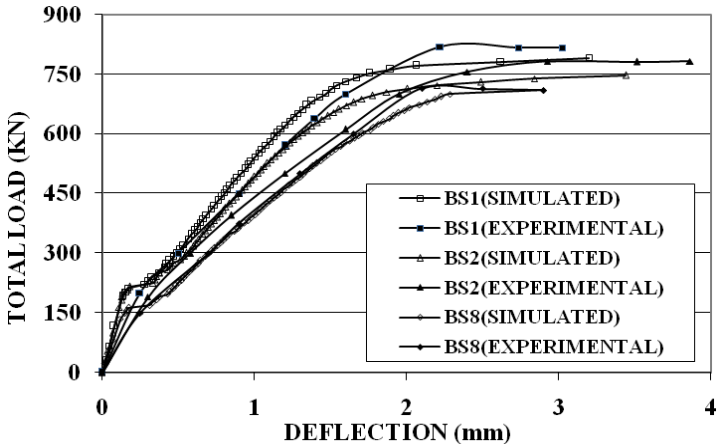

Fig. 14. Simulated and Experimental Load-Deflection Curves for BS1, BS2, and BS8

All tested beams exhibited limited displacement ductility at failure. The degree of ductility varied depending on the (a/d) ratio where the lower (a/d) ratio, the lower is amount of ductility. Increasing either vertical or horizontal shear reinforcement led to an increase in the analytical load carrying capacity and ductility matching with the experimental results. Increasing the concrete compressive strength has a significant improvement effect on the load-deflection response and there is an increase in the first flexural cracking, first diagonal cracking, and ultimate loads.

5- CONCLUSIONS

From the experimental and the analytical studies in the present work, the following conclusions are drawn:

1- Deep RC beams with smaller (a/d) ratio exhibit higher load carrying capacity, less deformation, and lower ductility than that of higher (a/d) ratio. Increasing concrete compressive strength leads to a more brittle behavior with increased

load carrying capacity and stiffness at different levels. Deep RC beams with different variables developed the same mode of failure. The failure planes were traced along the diagonal crack formed along the edges of load and intermediate support plates.

2- Tensile strains in bottom flexural reinforcement were higher than in top flexural steel due to internal stress redistribution. The lower the (a/d) ratio, the less variation is observed. For the vertical web reinforcement, a major redistribution of strains occurred for tested deep beams with (a/d) > 1 only. For the horizontal web reinforcement, major strain redistribution occurred for beams with (a/d) < 1.

3- The ultimate shear strength of continuous beams increases significantly with the decrease of the (a/d) ratio, and the increase of concrete compressive strength or vertical web reinforcement. The shear capacity of horizontal web steel was more prominent in continuous beams than that in simple ones, especially for beams with (a/d) < 1. Due to the limited internal redistribution of forces, the support reaction at interior support is slightly lower than that predicted by linear analysis.

4- The comparison between the obtained experimental results and the predictions of the ACI-318-08 and ECP-203-2007 codes indicated that current design codes underestimate the shear capacity of continuous deep beams. This may be attributed to the fact that the shear strength equation in both codes was derived from simple deep beams tests. Contrary to testing results, current design methods predict that shear resistance of horizontal web steel is higher than that of vertical steel.

5- The predictions of load-deflection response as well as the cracking patterns using the nonlinear finite element program, ANSYS 10, show a good agreement with the testing results. The finite element predicted successfully the ultimate loads, displacement ductility, stiffness changes and failure mechanisms for deep RC beams with different variables.

REFERENCES

1. Tuchscherer, R., Birrcher, D., and Bayrak, O., "Distribution of Stirrups across Web of Deep Beams", ACI Structural Journal, V. 108, No. 1, Jan.-Feb. 2011, pp. 108-115.

2. Hong, S. H., Hong, N. K., and Jang, S. K., "Deformation Capacity of Structural Concrete in Disturbed Regions", ACI Structural Journal, V. 108, No. 3, May-Jun. 2011, pp. 267-276.

3. Yank, K. H., "Tests on Lightweight Concrete Deep Beams", ACI Structural Journal, V. 107, No. 6, Nov.-Dec. 2010, pp. 663-670.

4. Mihaylov, B., Bentz, E. C., and Collins, M. P., "Behavior of Large Deep Beams Subjected to Monotonic and Reversed Cyclic Shear", ACI Structural Journal, V. 107, No. 6, Nov.-Dec. 2010, pp. 726-734.

5. Nathan, C. R., and Sergio, F. B., "Behavior of Deep Beams with Short Longitudinal Bar Anchorages", ACI Structural Journal, V. 105, No. 4, Jul.-Aug. 2008, pp. 460-470.

6. Ashour, A. F., and Yang, K. H., "Influence of Inclined Web Reinforcement on Reinforced Concrete Deep Beams with Openings", ACI Structural Journal, V. 104, No.5, Sep.-Oct. 2007, pp. 580-589.

7. Brown, M. D., and Bayark, O., "Investigation of Deep Beams with Various Load Configurations", ACI Structural Journal, V. 104, No.5, Sep.-Oct. 2007, pp. 611-620.

8. Yang, K. H., Eun, H. C., and Chung, H. S., "The Influence of Web Openings on the Structural Behavior of Reinforced High-Strength Concrete Deep Beams", Engineering Structures, V. 28, No. 13, 2006, pp. 1825-1834.

9. Yang, K., Chung, H., Lee, E., and Eun, H., "Shear Characteristics of High-Strength Concrete Deep Beams without Shear Reinforcements", Engineering Structures, V. 25, 2003, pp. 1343-1352.

10. Matsuo, M., Lertsrisakulrat, T., Yanagawa, A., and Niwa, J., "Shear Behavior of RC Deep Beams with Stirrups", Transactions of the Japan Concrete Institute, V. 23, 2002, pp. 385-390.

11. Yang, K. H., "Evaluation on the Shear Strength of High-Strength Concrete Deep Beams", PhD Thesis, Chungang University, Korea, Feb. 2002, 120 pp.

12. Ashour, A. F., Yang, K. H., "Effectiveness of Web Reinforcement around Openings in Continuous Concrete Deep Beams", ACI Structural Journal, V. 105, No.4, Jul-Aug. 2008, pp. 414-424.

13. Ashour, A. F., and Yang, K. H., "Influence of Shear Reinforcement on Reinforced Concrete Continuous Deep Beams", ACI Structural Journal, V. 104, No.4, Jul.-Aug. 2007, pp. 420-429.

14. Singh, S. K., Kaushik, K. F., and Sharma, N. S., "Design of a Continuous Deep Beam Using the Strut-and-Tie Method", Asian Journal of Civil Engineering, V. 7, No.5, 2006, pp. 461-477.

15. Ashour, A. F., and Rishi, G., "Tests of Reinforced Concrete Continuous Deep Beams with Web Openings", ACI Structural Journal, V. 97, No.8, May-Jun. 2000, pp. 418-426.

16. Walraven, J. C., "The Behavior of Reinforced Concrete Continuous Deep Beams", PhD Thesis, Delft University Press, Netherlands, Jan. 2000.

17. Mustafa, T.S., "Behavior of Reinforced Concrete Continuous Deep Beams ", PhD Thesis to be submitted, Faculty of Engineering at Shoubra, Benha University, Egypt, 2012.

18. ACI Committee 318, "Building Code Requirements for Structural Concrete (ACI 318-08) and Commentary (ACI 318-R-08)", ACI, Farmington Hills, 2008, 465 pp.

19. Egyptian Code of Practice ECP 203-2007, "Design and Construction of Reinforced Concrete Structures", Ministry of Building Construction, 2007.